ARTICLE

A Phospho-Directed Macroporous Alumina–Silica Nanoreactor with Multi-Functions

Kun Qian,[†] Jingjing Wan,[†] Fang Liu,[†] Hubert H. Girault,[‡] Baohong Liu,[†,*] and Chengzhong Yu[†,§,*]

[†]Department of Chemistry, Institute of Biomedical Sciences, and Shanghai Key Laboratory of Molecular Catalysis and Innovative Materials, Fudan University, Shanghai 200433, People's Republic of China, [‡]Laboratoire d'Electrochimie Physique et Analytique, Ecole Polytechnique Fédérale de Lausanne, Station 6, CH-1015 Lausanne, Switzerland, and [§]ARC Centre of Excellence for Functional Nanomaterials and Australian Institute for Bioengineering and Nanotechnology, The University of Queensland, Brisbane QLD 4072, Australia

ABSTRACT A phospho-directed nanoreactor with multiple functions is reported. Alumina-functionalized macroporous ordered silica foams (Al-MOSF) have been developed with large pore size, high pore volume (1.6 cm^3/g), and a surface area of 186 m^2/g rich in coordination unsaturated Al species, which can be used as phospho-directed nanoreactors for integrated *in situ* digestion and *in situ* phosphoisolation. By directly adding Al-MOSF to the conventional in-solution digestion system, both enzymes and proteins are quickly enriched in the macropores of the reactor to achieve a fast proteolysis without increasing the enzyme/protein concentration or using a preimmobilization process, thus the digestion time and the cost can be greatly reduced. Meanwhile, due to the chemo-affinity between alumina and phosphor groups, the Al-MOSF reactor can *in situ* isolate specific products of the enzymatic reaction (*i.e.*, phosphopeptides) and release the nonspecific peptides to the solution. This strategy is simple, efficient, and successfully applied in the detection of phosphoproteins in real samples.

KEYWORDS: phosphoprotein · macroporous · alumina–silica · nanoreactor · digestion

Nanomaterials with designed structures and functions have been widely used in a range of biological applications.[1−3] With the development of state-of-the-art nanotechniques,[4,5] various nanoreactors with high-throughput and ultrasensitivity have been fabricated and have found applications in sensors,[6−9] drug delivery,[10,11] and crystal growth.[12,13] Currently, many micro/nanoreactors are designed to meet the urgent demand of efficient enzymatic reactions,[14−22] which is fundamentally important to understand the life bioactivities in confined organelle and also a key procedure in the mass spectrometry (MS)-based proteomics.[23] Despite the tremendous recent success, the function of developed nanoreactors in modern proteomics is focused principally on accelerating the enzymatic reaction kinetics and thus it is difficult to achieve multiple functions. A new concept of nanoreactor with integrated multi-functions and universal applications needs to be developed in terms of the rising challenges in the large-scale proteomic research toward proteins with specific chemo groups in the post-translational modifications (PTMs).[24,25]

As one of the most important PTMs, reversible protein phosphorylation regulates a majority of biological processes.[26−28] Numerous efforts have been dedicated to investigate phosphoprotein through MS technique as a primary choice.[29] Various phosphorylated proteins exist in cells; however, the characterization of substoichiometric phosphorylation is still a challenging task. Many phosphoproteins are hard to be digested and analyzed[23,30] because many of them targeted for phosphorylation remain at very low concentrations physiologically and complex in nature.[31] Although substantial progress has been made in phosphopeptide enrichment,[29,32−34] most of current strategies require multiple procedures including time-consuming and labor-intensive predigestion of phosphoproteins, then enrichment and post-isolation of target phosphopeptides. An advanced nanoreactor that can combine the above functions in one pot is thus of great importance, which has not been reported until now.

Mesoporous materials have been demonstrated to be good candidates for nanoreactors.[19,35,36] Benefiting from their relatively large pore sizes and high pore volumes, mesoporous materials were employed to preimmobilize high concentration of enzymes (or proteins) within the nanopores to fasten the enzymatic reaction rate and reduce the digestion time. However, the success is at the expense of increasing the amount of expensive enzymes/proteins, and such a preimmobilization process is also not convenient for

*Address correspondence to czyu@fudan.edu.cn, bhliu@fudan.edu.cn.

Received for review July 5, 2009 and accepted October 14, 2009.

Published online October 20, 2009. 10.1021/nn900739z CCC: $40.75

© 2009 American Chemical Society

practical operations. More importantly, because pure silica does not have desired interactions with the target chemo groups in proteins with specific PTMs or specific peptides, such nanoreactors cannot achieve multi-functions without rational surface modification.[19,35,36]

Previously, we reported the synthesis of macroporous ordered silica foams (MOSF) *via* a supra-assembly approach using cooperative self-assembled vesicles as building blocks.[37] The formation of MOSFs is governed by the surface area minimization rule, similar to the packing model of bubble-like soft materials.[38] By surface modification of MOSF with TiO_2 species, functionalized Ti-MOSF materials with large surface area and quantities of binding sites were demonstrated to be effective in the enrichment of phosphopeptides.[39] It is hypothesized that, by further taking advantage of the very large macropores, MOSF materials with designed surface properties can be used as a nanoreactor with enhanced functions in PTM study.

Herein, we report the synthesis and characterization of Al-MOSF based on the surface modification of MOSF materials by alumina, which can be used as a multi-functional phospho-directed nanoreactor (Scheme 1A). As shown in Scheme 1B, by directly adding Al-MOSF into a standard digestion system (without increasing the amount of enzymes), the digestion of proteins and the enrichment of phosphopeptides as well as further isolation process can be completed in one pot within 30 min, in great contrast to conventional methods where in-solution predigestions (generally 6−24 h) and multiple procedures for subsequent enrichment and isolation processes are needed. The mechanism of phospho-directed nanoreactors is shown in Scheme 1A. Al-MOSF with very large pores and high pore volumes (1.6 cm^3/g) has ultrafast immobilization kinetics and high capacity for both enzymes and proteins. After adding Al-MOSF to the conventional digestion system, enzymes/proteins can be *in situ* enriched in the nanopores of Al-MOSF promptly with a high local concentration to undergo a fast nanodigestion. At the same time, due to the chemo-affinity between alumina and phosphate groups, the specific phosphopeptides can be *in situ* adsorbed in the Al-MOSF, while the non-specific digestion products (non-phosphopeptides) were mainly released to the solutions. As a result, the enriched phosphopeptides can be simply detected. Furthermore, the Al-MOSF nanoreactor can be applied to achieve a very low detection limit in the analysis of complex samples.

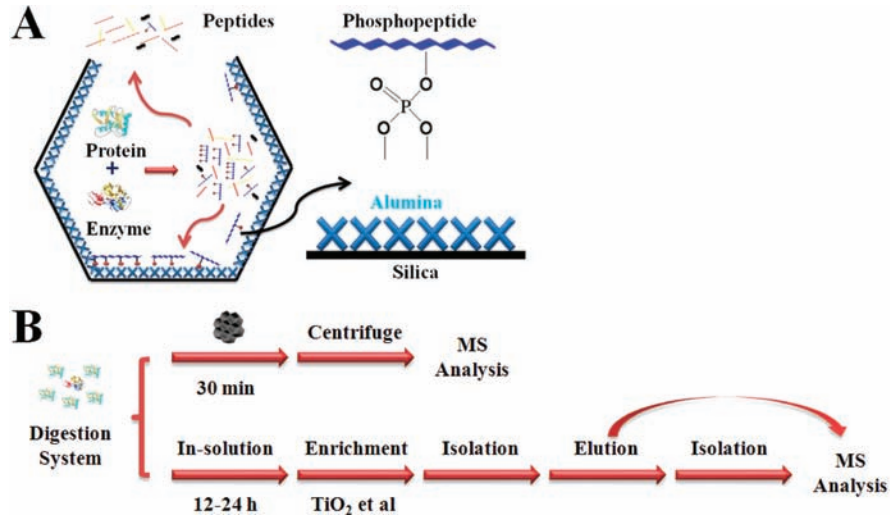

Scheme 1. (A) Illustration of the structure and mechanism of the Al-MOSF nanoreactor. (B) Comparison between the overall strategy of our approach (upper) and traditional pathways (below).

RESULTS AND DISCUSSION

Figure 1 displays the scanning electron microscopy (SEM) images of MOSF and Al-MOSF materials. Macropores with ~100 nm diameter can be clearly observed for both materials, indicating that the foam-like structure of MOSF can be well-preserved after surface modification with alumina. Under SEM observation, no aggregated alumina are found in Al-MOSF materials, suggesting that the alumina species exist in a well-dispersed state in Al-MOSF. The final Si/Al molar ratio is 5/1 according to the energy-dispersive X-ray (EDX) spectrometry analysis results. The nitrogen sorption analysis is carried out for both MOSF and Al-MOSF materials shown in Figure SI-1 in the Supporting Information. The surface area and pore volume of MOSF materials are 276 m^2/g and 2.2 cm^3/g, respectively. After functionalization with alumina, Al-MOSF materials possess a surface area of 186 m^2/g and a pore volume of 1.6 cm^3/g. The decrease in surface area and pore volume of Al-MOSF can be attributed to the incorporation of Al_2O_3 (with a relatively higher density of ~3.9 cm^3/g) within the SiO_2 matrix (with a relatively lower density of ~2.2 cm^3/g). The pore size distribution curves calculated from the adsorption branch using the Broekhoff−de Boer (BdB) model show a maximum at ~75 and 70 nm for MOSF and Al-MOSF, respectively (Figure SI-2 in the Supporting Information). Although

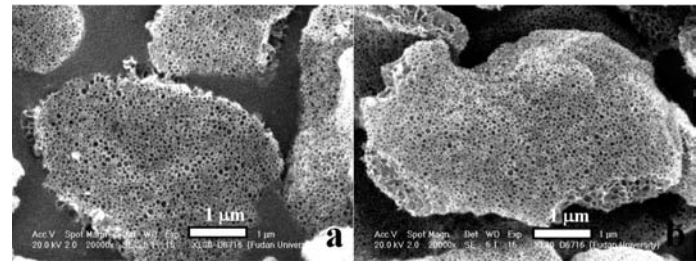

Figure 1. SEM images of the wasp-nest-like MOSF materials (a) and Al-MOSF nanoreactors (b).

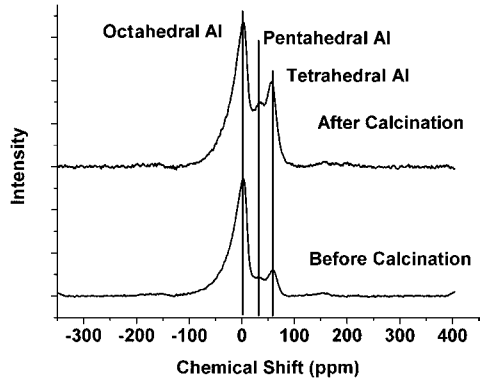

Figure 2. Solid-state MAS ^{27}Al NMR spectrum of Al-MOSF nanoreactors before and after calcinations.

the macropore size cannot be accurately measured by the N_2 sorption analysis, it is still possible to estimate that the macroporous structure of MOSF is well-preserved after alumina modification process, in agreement with the SEM observations.

Solid state ^{27}Al nuclear magnetic resonance (NMR) spectra of Al-MOSF materials both before and after baking treatment at 500 °C are displayed in Figure 2. For both materials, three distinct peaks with maxima centered at 4, 32, and 56 ppm are observed, which can be assigned to octahedral, pentahedral, and tetrahedral Al species, respectively.[40,41] The obtained spectra for both materials are clearly different from that for a conventional γ-Al_2O_3 because the spectrum of the latter shows predominately octahedral and tetrahedral Al species, while no contribution from pentahedral Al species is observed.[40,41] Meanwhile, the chemical shift of the tetrahedral Al peak (56 ppm) is lower than that of bulk γ-Al_2O_3 (65 ppm) and close to that of tetrahedral Al species in zeolites and amorphous silica−alumina composites, suggesting the formation of Al−O−Si bonds resulting from the incorporation of Al atoms within the SiO_2 framework of MOSF.[40−42] After deconvolution, the percentages of pentahedral and tetrahedral Al species in terms of the total aluminum species for Al-MOSF before baking are determined to be 6.50 and 12.85%, respectively. After the baking treatment at 500 °C for 5 h, the percentages of pentahedral and tetrahedral Al species increase to 22.85 and 35.51%, respectively. It is concluded that, due to the dehydration of alumina and further Si−O−Al bond formation at high temperature, the baking process is advantageous for the generation of high percentages of Al species with unsaturated coordination states, which is crucial for the following phosphopeptide enrichment.[39,43]

The ζ potentials of both MOSF and Al-MOSF materials are also measured in the ammonium bicarbonate solution (25 mM, pH ~8). As shown in Figure 3, the ζ potential of MOSF is measured to be −33.9 mV, whereas for Al-MOSF, the ζ potential is increased to −6.8 mV, in accordance with previous reports for the surface modification of silica with alumina species.[44,45] In addition,

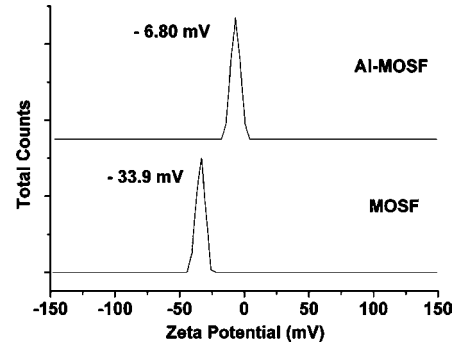

Figure 3. Zeta potential distributions of MOSF and Al-MOSF.

only one narrow peak is observed for Al-MOSF (−6.8 mV), and the peak at −33.9 mV for MOSF cannot be observed after alumina modification, considering that alumina has a higher isoelectric point (pI) of ~9.8 compared to silica (pI ~2).[45] The above observations as well as the SEM, N_2 sorption, and ^{27}Al NMR results have shown that the pure silica surface of MOSF has been successfully functionalized into alumina species for Al-MOSF, and Al-MOSF has very large pore size, high pore volume, and a large area of functionalized surface with coordination of unsaturated Al species.

To further study the potential of Al-MOSF as a nanoreactor in the enzymatic reaction, the immobilization and the capacity of protein/enzyme in Al-MOSF were studied. For a phosphoprotein, β-casein, ~98% of the maximum adsorption amount can be achieved in less than 1 min (as shown in Figure 4a). Moreover, the immobilization capacity of β-casein

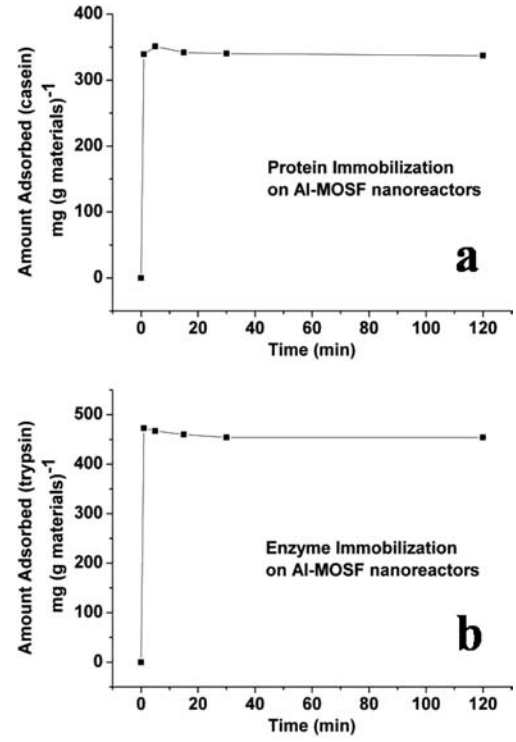

Figure 4. Adsorption of (a) proteins and (b) enzymes into Al-MOSF nanoreactors as a function of time.

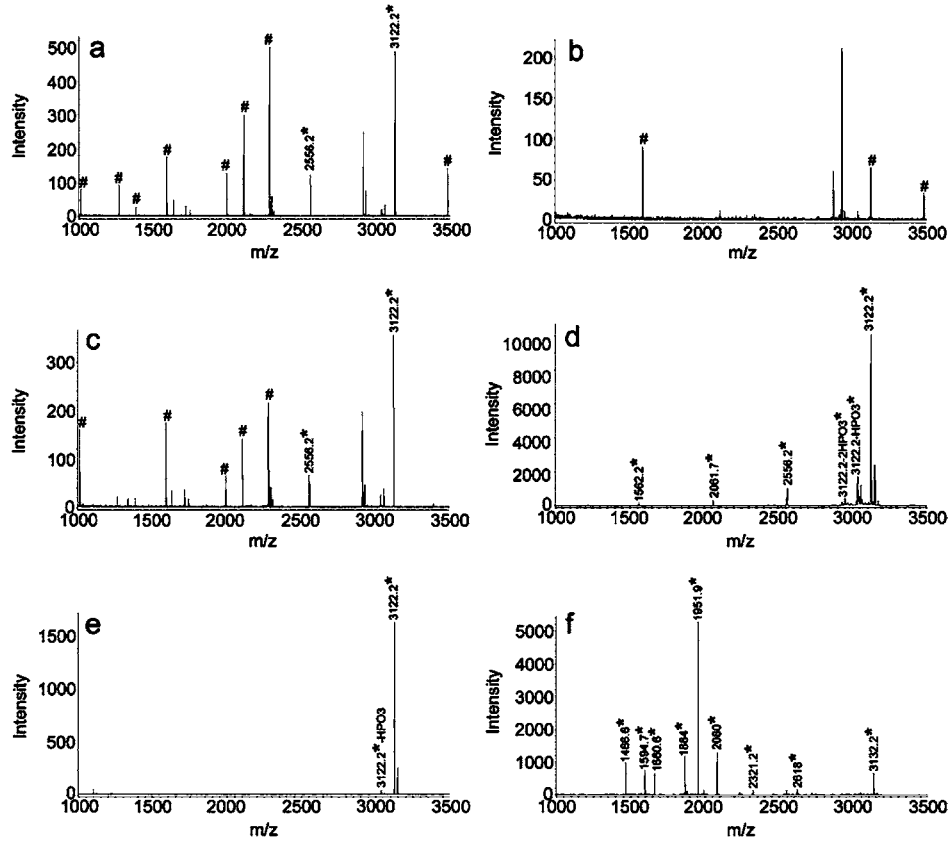

Figure 5. Mass spectra of proteolysis products from (a) 30 min Al-MOSF-catalyzed β-casein (20 ng/μL) digestion, (b) 30 min in-solution β-casein (20 ng/μL) digestion, (c) 12 h in-solution β-casein (20 ng/μL) digestion; and mass spectra of the separated nanoreactors obtained from 30 min Al-MOSF-catalyzed (d) 20 ng/μL, (e) 2 ng/μL β-casein, (f) 20 ng/μL α-casein digestion. The peaks marked with an asterisk are for phosphopeptides, while # represents the non-phosphopeptides. Detailed information of the identified phosphopeptides can be found in Table SI-1 in the Supporting Information.

is 350 mg (g Al-MOSF)$^{-1}$. In the case of trypsin, an enzyme generally used to digest proteins, the immobilization capacity adsorbed in Al-MOSF is 460 mg (g Al-MOSF)$^{-1}$. Similarly, the maximum immobilization capacity is obtained within 1 min (Figure 4b). In a typical digest system, the concentration of the protein (β-casein) is as low as 0.02 mg/mL. It is not convenient to measure the immobilization capacity of β-casein in Al-MOSF at such a low concentration. Nevertheless, considering the large immobilization capacity of β-casein in Al-MOSF (350 mg/g) measured at a higher β-casein concentration (1 mg/mL), it can be roughly estimated that an Al-MOSF concentration of ~0.06 mg/mL should be used. In our further digest experiments, the Al-MOSF concentration is increased to 0.13 mg/mL in order to immobilize the maximum amount of proteins into Al-MOSF (see Methods section). Assuming that the majority of β-casein can be quickly absorbed from in-solution into the macropores of Al-MOSF, a concentration increase of ~4800 times can be calculated. Because the immobilization capacity of trypsin in Al-MOSF is also high (460 mg/g) and the weight ratio of trypsin to β-casein is 1:30, the relatively smaller amount of trypsin can also be adsorbed quickly into Al-MOSF. It is expected that the *in situ* enrichment of proteins and enzymes into Al-MOSF may greatly enhance the effective collision between biomolecules and increase the enzymatic reaction kinetics. Moreover, the high surface area of functionalized Al-MOSF can be used to selectively capture phosphopeptides after digestion. Thus, Al-MOSF can be used as a multifunctional nanoreactor in not only enzymatic reaction but also the selectively enrichment of phosphopeptides.

The performance of the Al-MOSF nanoreactor with multiple functions has been tested by the analysis of β-casein using the matrix-assisted laser desorption/ionization time-of-flight mass spectrometry (MALDI-TOF MS). First, we studied the function of the Al-MOSF nanoreactor to accelerate the protein digestion. Figure 5a−c displays the peptide mass fingerprinting (PMF) spectra of β-casein digest (20 ng/μL) with different methods. As shown in Figure 5a, 10 peptides are observed after digestion by directly adding Al-MOSF (0.13 mg/mL) in the digestion system for 30 min. For comparison, only three peptides are observed in the case of the standard in-solution digestion for 30 min (Figure 5b). For the standard overnight (12 h) in-solution digestion, seven peptides are detected in the mass spectrum (Figure 5c). By comparing the above results, it is confirmed that

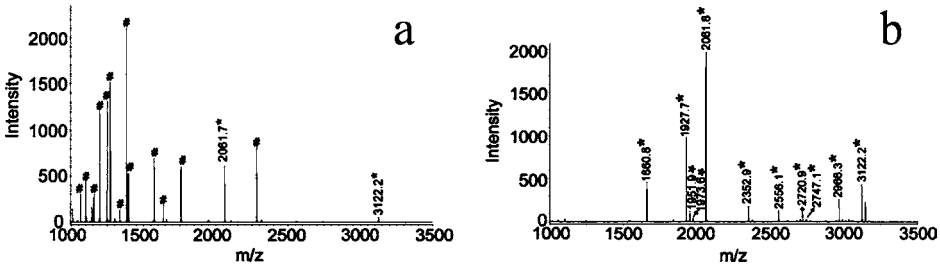

Figure 6. PMF spectra of 20 ng/μL bovine milk from (a) in-solution digested in 24 h and (b) separated Al-MOSF nanoreactors after nanodigestion and phosphoisolation for 30 min; the peaks marked with asterisk are for phosphopeptides, while # represents the non-phosphopeptides.

Al-MOSF can be used as a nanoreactor to largely enhance the digestion efficiency and greatly reduce the digestion time.

Besides the highly efficient proteolysis, the Al-MOSF can also perform *in situ* specific enrichment toward phosphopeptides meanwhile considering the chemo-affinity of coordination unsaturated alumina species toward the phospho groups.[46] After the effective digestion, Al-MOSF was separated and detected by the MALDI-TOF MS. As shown in Figure 5d, three phosphopeptides obtained from β-casein with mass/charge (*m/z*) of 2061.7, 2556.2, and 3122.2 dominate the mass spectrum. The tetraphosphorylated peptide signal (*m/z* of 3122.3) takes a majority place in the mass spectrum, and the dephosphorylated fragments of tetraphosphorylated peptide (*m/z* of 3042.2, 2962.2) can also be observed. The results show that a multi-functional nanoreactor combining ultrafast digestion and specific enrichment of target peptides can be realized, which largely reduce the reaction time and show great potentials in the high-throughput proteomic research. The multi-functions of Al-MOSF were further investigated in the detection of β-casein at a low concentration of 2 ng/μL. As shown in the mass spectrum (Figure 5e), the peak at *m/z* of 3122.2 as well as the dephosphorylated fragments (*m/z* of 3042.2) can be observed with a high signal-to-noise. The concept of using Al-MOSF as a multi-functional
nanoreactor in the phosphoprotein analysis is further testified by the detection of another phosphorylated protein α-casein. Similarly, the *in situ* digestion of the α-casein (20 ng/μL) and phophopeptide enrichment are completed in the nanoreactor within 30 min. The mass spectrum displays that nine phosphopeptides including single and multiple phosphorylated species are captured by the Al-MOSF and no non-phosphopeptides are observed (Figure 5f).

Our approach is further applied in the analysis of biosamples to digest and enrich phosphopeptides from the commercial nonfat bovine milk. Figure 6a presents a MALDI mass spectrum of the sample treated by the 24 h tryptic digestion. Only two weak signals of phosphopeptides at *m/z* of 2061.8 and 3122.2 appear together with abundant non-phosphopeptide signals. However, by adding Al-MOSF into the bovine milk digest solution for only 30 min, we can see that all of the nine dominating peaks observed in Figure 6b are attributed to phosphorylated peptides, including six peptides generated from α-casein and the other three from β-casein. The above results have demonstrated the strong potential of Al-MOSF nanoreacror toward the phospho-analysis of a complex sample.

CONCLUSIONS

In summary, an alumina-functionalized macroporous material Al-MOSF has been successfully synthesized and used as a phospho-directed nanoreactor with multiple functions, which combine the *in situ* proteolysis and enrichment *via* one simple integrated step but with high efficiency. By directly adding Al-MOSF to the conventional digestion system, the proteins/enzymes can be enriched in the nanopores quickly to greatly reduce the digestion time. Meanwhile, the specific phosphopeptides are enriched in the nanoreactor due to the chemo-affinity between phospho groups and alumina. As a result, our strategy using Al-MOSF nanoreactor provides a simple, cheap, and efficient solution compared to previous methods. The phospho-directed nanoreactor has been demonstrated to be effective for not only standard phosphoproteins but also biocomplex samples. It is anticipated that, by the rational design of functional macroporous materials, versatile nanoreactors with enhanced multi-functions and desired selectivity can be fabricated, which may find applications in enzymatic catalysis and modern proteomics.

METHODS

Chemicals. Tetramethoxysilane (TMOS), $EO_{20}PO_{70}EO_{20}$ [denoted P123, where EO is poly(ethylene oxide) and PO is poly(propylene oxide)], aluminum isopropoxide and ammonium bicarbonate were purchased from Aldrich. Trypsin (from bovine pancreas), α-casein (from bovine milk, 90%), and β-casein (from bovine milk, 90%) were obtained from Sigma. 2,5-Dihydroxybenzoic acid (DHB, 99.9%), acetonitrile (ACN, 99.9%), and trifluoroacetic acid (TFA, 99.8%) were purchased from Merck. All reagents were used as received without further purification. Deionized water (18.4 MΩ · cm) used for all experiments was obtained from a Milli-Q system (Millipore, Bedford, MA).

Synthesis and Characterization of Materials. Pure silica MOSF materials were synthesized according to our previous report.[37] Typically, the synthesis was carried out at 35 °C in a buffer solution

(pH of 5) with TMOS as a silica source and P123 as a template. The final MOSF products were obtained after calcination at 550 °C for 5 h. For the modification of MOSF with alumina, 0.3 g of aluminum isopropoxide was dissolved in 30 mL of toluene. Then 0.1 g of calcined MOSF was added, dispersed, and refluxed at 110 °C for 8 h. The mixture was then filtered and washed by toluene and ethanol three times. The resulting materials were dried and baked at 500 °C in air for 5 h to obtain the final Al-MOSF material.

Scanning electron microscopy (SEM) images were recorded on a JEOL 6400 microscope operating at 10 kV, and the samples were coated with gold. The element molar ratio was measured by the energy-dispersive X-ray (EDX) spectroscopy. Nitrogen sorption isotherms of samples were obtained by a Quantachrome's Quadrasorb SI analyzer at 77 K. Before the measurements, the samples were degassed at 180 °C for 6 h in vacuum. The magic angle spinning (MAS) ^{27}Al NMR spectra were recorded on a Bruker DSX 300 NMR spectrometer operating at a resonance frequency of 78.2 MHz (0.3 μs as a pulse width). A ζ potential meter (Malvern Zetasizer Nano) was used to measure the ζ potentials of materials at 298 K in pH = 8 ammonium bicarbonate buffer solution.

Immobilization of Proteins/Enzymes into Al-MOSF. For the immobilization test, 2.0 mg of Al-MOSF was added into 4 mL of protein solution (1 mg/mL) in the ammonium bicarbonate buffer (25 mM, pH ~8.0). The mixture was stirred at 298 K for different time to reach the adsorption maximum. The adsorbed amount was measured using a difference method with protein concentrations determined before and after adsorption by UV absorption at 280 nm on a V-550 UV/vis spectrophotometer.

Digestion and Isolation of Phospho Species for MALDI-TOF MS Analysis. For in-solution digestion, 1 mg of α-casein or β-casein was dissolved in 1 mL of ammonium bicarbonate (25 mM, pH ~8) separately, denatured at 100 °C for 5 min and digested for overnight (12−24 h) at 37 °C with an enzyme to protein ratio of 1:30 (w/w). For the digestion in the presence of Al-MOSF, 2 μL of 20 mg/mL Al-MOSF was directly added into 300 μL of α-casein or β-casein in-solution digestion system (20 ng/μL or 2 ng/μL) and incubated at 37 °C for 30 min. For the biosample, 30 μL of bovine milk was diluted in 900 μL of NH_4HCO_3 aqueous solution at 25 mM. This solution was then centrifugated at 16 000 rpm for 15 min, and the supernatant was collected for tryptic digestion.

After the digestion, the mixture was centrifugated to separate the deposits and the supernatant followed by MALDI-TOF MS detection of two parts individually. The deposits were washed by a solution of 0.1% TFA (50% ACN/water) 20 μL two times. Finally, 10 μL of 0.1% TFA (50% ACN/water) was added to the deposits, and the suspension (1 μL) was directly deposited on the MALDI plate. After evaporation of the solvent, 0.5 μL of DHB (10 mg/mL in 50% ACN/water, 1% H_3PO_4) was added and dried at room temperature. The MALDI-TOF MS experiments were performed on a Bruker Microflex equipped with a nitrogen laser operated at 337 nm. The data analysis and peptide sequence were performed using the flex Analysis software from Bruker.

Acknowledgment. This work is supported by 973 Program (2010CB226901, 2006CB932302, 2007CB714506), NSFC (20721063, 20775016, 20925517), SLADP (B108, B109), Shanghai STC (07QH1400308, DZ2270500, 09JC1402600), Shuguang 06SG02, FANEDD (200423), and the Ministry of Education of China (20060246010). J.W. is grateful to EPFL for a visiting fellowship.

Supporting Information Available: Nitrogen adsorption isotherms and pore size distributions of MOSF and Al-MOSF, and detailed information of the observed phosphorylated peptides. This material is available free of charge *via* the Internet at http://pubs.acs.org.

REFERENCES AND NOTES

1. Peer, D.; Park, E. J.; Morishita, Y.; Carman, C. V.; Shimaoka, M. Systemic Leukocyte-Directed siRNA Delivery Revealing Cyclin D1 as an Anti-inflammatory Target. *Science* **2008**, *319*, 627–630.
2. Anderson, D. G.; Levenberg, S.; Langer, R. Nanoliter-Scale Synthesis of Arrayed Biomaterials and Application to Human Embryonic Stem Cells. *Nat. Biotechnol.* **2004**, *22*, 863–866.
3. Luckarift, H. R.; Spain, J. C.; Naik, R. R.; Stone, M. O. Enzyme Immobilization in a Biomimetic Silica Support. *Nat. Biotechnol.* **2004**, *22*, 211–213.
4. LaVan, D. A.; McGuire, T.; Langer, R. Small-Scale Systems for *In Vivo* Drug Delivery. *Nat. Biotechnol.* **2003**, *21*, 1184–1191.
5. Whitesides, G. M. The 'Right' Size in Nanobiotechnology. *Nat. Biotechnol.* **2003**, *21*, 1161–1165.
6. Broz, P.; Driamov, S.; Ziegler, J.; Ben-Haim, N.; Marsch, S.; Meier, W.; Hunziker, P. Toward Intelligent Nanosize Bioreactors: A pH-Switchable, Channel-Equipped, Functional Polymer Nanocontainer. *Nano Lett.* **2006**, *6*, 2349–2353.
7. Wang, Z. G.; Shang, H.; Lee, G. U. Nanoliter-Scale Reactor Arrays for Biochemical Sensing. *Langmuir* **2006**, *22*, 6723–6726.
8. Rusling, J. F.; Hvastkovs, E. G.; Schenkman, J. B. Toxicity Screening Using Biosensors That Measure DNA Damage. *Curr. Opin. Drug Discovery Dev.* **2007**, *10*, 67–73.
9. Muraviev, D. N.; Macanas, J.; Esplandiu, M. J.; Farre, M.; Munoz, M.; Alegret, S. Simple Route for Intermatrix Synthesis of Polymer Stabilized Core−Shell Metal Nanoparticles for Sensor Applications. *Phys. Status Solidi A* **2007**, *204*, 1686–1692.
10. Ranquin, A.; Versees, W.; Meier, W.; Steyaert, J.; Van Gelder, P. Therapeutic Nanoreactors: Combining Chemistry and Biology in a Novel Triblock Copolymer Drug Delivery System. *Nano Lett.* **2005**, *5*, 2220–2224.
11. Gupta, V.; Gupta, R.; Grover, R.; Khanna, R.; Jangra, V.; Mittall, A. Delivery of Molecules to Cancer Cells Using Liposomes from Bacterial Cultures. *J. Nanosci. Nanotechnol.* **2008**, 2328–2333.
12. Lee, S. Y.; Gao, X. Y.; Matsui, H. Biomimetic and Aggregation-Driven Crystallization Route for Room-Temperature Material Synthesis: Growth of Beta-Ga_2O_3 Nanoparticles on Peptide Assemblies as Nanoreactors. *J. Am. Chem. Soc.* **2007**, *129*, 2954–2958.
13. de la Rica, R.; Matsui, H. Urease as a Nanoreactor for Growing Crystalline ZnO Nanoshells at Room Temperature. *Angew. Chem., Int. Ed.* **2008**, *47*, 5415–5417.
14. Liu, Y.; Xue, Y.; Ji, J.; Chen, X.; Kong, J.; Yang, P. Y.; Girault, H. H.; Liu, B. H. Gold Nanoparticle Assembly Microfluidic Reactor for Efficient On-line Proteolysis. *Mol. Cell. Proteomics* **2007**, *6*, 1428–1436.
15. Qian, K.; Wan, J.; Qiao, L.; Huang, X.; Tang, J.; Wang, Y.; Kong, J.; Yang, P.; Yu, C.; Liu, B. Macroporous Materials as Novel Catalysts for Efficient and Controllable Proteolysis. *Anal. Chem.* **2009**, *81*, 5749–5756.
16. Bruns, N.; Tiller, J. C. Amphiphilic Network as Nanoreactor for Enzymes in Organic Solvents. *Nano Lett.* **2005**, *5*, 45–48.
17. Neumann, T.; Haupt, B.; Ballauff, M. High Activity of Enzymes Immobilized in Colloidal Nanoreactors. *Macromol. Biosci.* **2004**, *4*, 13–16.
18. Fang, M.; Grant, P. S.; McShane, M. J.; Sukhorukov, G. B.; Golub, V. O.; Lvov, Y. M. Magnetic Bio/Nanoreactor with Multilayer Shells of Glucose Oxidase and Inorganic Nanoparticles. *Langmuir* **2002**, *18*, 6338–6344.
19. Qiao, L.; Liu, Y.; Hudson, S. P.; Yang, P. Y.; Magner, E.; Liu, B. H. A Nanoporous Reactor for Efficient Proteolysis. *Chem.—Eur. J.* **2008**, *14*, 151–157.
20. Liu, Y.; Zhong, W.; Meng, S.; Kong, J. L.; Lu, H. J.; Yang, P. Y.; Girault, H. H.; Liu, B. H. Assembly-Controlled Biocompatible Interface on a Microchip: Strategy to Highly Efficient Proteolysis. *Chem.—Eur. J.* **2006**, *12*, 6585–6591.
21. Liu, Y.; Lu, H. J.; Zhong, W.; Song, P. Y.; Kong, J. L.; Yang, P. Y.; Girault, H. H.; Liu, B. H. Multi Layer-Assembled Microchip for Enzyme Immobilization as Reactor toward Low-Level Protein Identification. *Anal. Chem.* **2006**, *78*, 801–808.

22. Zhang, Y. H.; Liu, Y.; Kong, J. L.; Yang, P. Y.; Tang, Y.; Liu, B. H. Efficient Proteolysis System: A Nanozeolite-Derived Microreactor. *Small* **2006**, *2*, 1170–1173.
23. Cravatt, B. F.; Simon, G. M.; Yates, J. R. The Biological Impact of Mass-Spectrometry-Based Proteomics. *Nature* **2007**, *450*, 991–1000.
24. Ingmundson, A.; Delprato, A.; Lambright, D. G.; Roy, C. R. *Legionella pneumophila* Proteins that Regulate Rab1 Membrane Cycling. *Nature* **2007**, *450*, U365–U361.
25. Ptacek, J.; Devgan, G.; Michaud, G.; Zhu, H.; Zhu, X. W.; Fasolo, J.; Guo, H.; Jona, G.; Breitkreutz, A.; Sopko, R.; McCartney, R. R.; Schmidt, M. C.; Rachidi, N.; Lee, S. J.; Mah, A. S.; Meng, L.; Stark, M. J. R.; Stern, D. F.; De Virgilio, C.; Tyers, M.; Andrews, B.; Gerstein, M.; Schweitzer, B.; Predki, P. F.; Snyder, M. Global Analysis of Protein Phosphorylation in Yeast. *Nature* **2005**, *438*, 679–684.
26. Hume, A. J.; Finkel, J. S.; Kamil, J. P.; Coen, D. M.; Culbertson, M. R.; Kalejta, R. F. Phosphorylation of Retinoblastoma Protein by Viral Protein with Cyclin-Dependent Kinase Function. *Science* **2008**, *320*, 797–799.
27. Macurek, L.; Lindqvist, A.; Lim, D.; Lampson, M. A.; Klompmaker, R.; Freire, R.; Clouin, C.; Taylor, S. S.; Yaffe, M. B.; Medema, R. H. Polo-like Kinase-1 is Activated by Aurora A to Promote Checkpoint Recovery. *Nature* **2008**, *455*, U119–U188.
28. Pan, W. J.; Choi, S. C.; Wang, H.; Qin, Y. B.; Volpicelli-Daley, L.; Swan, L.; Lucast, L.; Khoo, C.; Zhang, X. W.; Li, L.; Abrams, C. S.; Sokol, S. Y.; Wu, D. Q. Wnt3a-Mediated Formation of Phosphatidylinositol 4,5-Bisphosphate Regulates LRP6 Phosphorylation. *Science* **2008**, *321*, 1350–1353.
29. Bodenmiller, B.; Mueller, L. N.; Mueller, M.; Domon, B.; Aebersold, R. Reproducible Isolation of Distinct, Overlapping Segments of the Phosphoproteome. *Nat. Methods* **2007**, *4*, 231–237.
30. Doucette, A.; Craft, D.; Li, L. Protein Concentration and Enzyme Digestion on Microbeads for MALDI-TOF Peptide Mass Mapping of Proteins from Dilute Solutions. *Anal. Chem.* **2000**, *72*, 3355–3362.
31. Aebersold, R.; Mann, M. Mass Spectrometry-Based Proteomics. *Nature* **2003**, *422*, 198–207.
32. Mazanek, M.; Mituloviae, G.; Herzog, F.; Stingl, C.; Hutchins, J. R. A.; Peters, J. M.; Mechtler, K. Titanium Dioxide as a Chemo-Affinity Solid Phase in Offline Phosphopeptide Chromatography Prior to HPLC-MS/MS Analysis. *Nat. Protoc.* **2007**, *2*, U1059–U1051.
33. Thingholm, T. E.; Jorgensen, T. J. D.; Jensen, O. N.; Larsen, M. R. Highly Selective Enrichment of Phosphorylated Peptides Using Titanium Dioxide. *Nat. Protoc.* **2006**, *1*, 1929–1935.
34. Qiao, L.; Roussel, C.; Wan, J. J.; Yang, P. Y.; Girault, H. H.; Liu, B. H. Specific On-Plate Enrichment of Phosphorylated Peptides for Direct MALDI-TOF MS Analysis. *J. Proteome Res.* **2007**, *6*, 4763–4769.
35. Fan, J.; Shui, W. Q.; Yang, P. Y.; Wang, X. Y.; Xu, Y. M.; Wang, H. H.; Chen, X.; Zhao, D. Y. Mesoporous Silica Nanoreactors for Highly Efficient Proteolysis. *Chem.—Eur. J.* **2005**, *11*, 5391–5396.
36. Shui, W. Q.; Fan, J.; Yang, P. Y.; Liu, C. L.; Zhai, J. J.; Lei, J.; Yan, Y.; Zhao, D. Y.; Chen, X. Nanopore-Based Proteolytic Reactor for Sensitive and Comprehensive Proteomic Analyses. *Anal. Chem.* **2006**, *78*, 4811–4819.
37. Wang, H. N.; Zhou, X. F.; Yu, M. H.; Wang, Y. H.; Han, L.; Zhang, J.; Yuan, P.; Auchterlonie, G.; Zou, J.; Yu, C. Z. Supra-Assembly of Siliceous Vesicles. *J. Am. Chem. Soc.* **2006**, *128*, 15992–15993.
38. Yuan, P.; Zhou, X. F.; Wang, H. N.; Liu, N. A.; Hu, Y. F.; Auchterlonie, G. J.; Drennan, J.; Yao, X. D.; Lu, G. Q.; Zou, J.; Yu, C. Z. Electron-Tomography Determination of the Packing Structure of Macroporous Ordered Siliceous Foams Assembled From Vesicles. *Small* **2009**, *5*, 377–382.
39. Wan, J. J.; Qian, K.; Qiao, L.; Wang, Y. H.; Kong, J. L.; Yang, P. Y.; Liu, B. H.; Yu, C. Z. TiO_2-Modified Macroporous Silica Foams for Advanced Enrichment of Multi-Phosphorylated Peptides. *Chem.—Eur. J.* **2009**, *15*, 2504–2508.
40. Baca, M.; de la Rochefoucauld, E.; Ambroise, E.; Krafft, J. M.; Hajjar, R.; Man, P. P.; Carrier, X.; Blanchard, J. Characterization of Mesoporous Alumina Prepared by Surface Alumination of SBA-15. *Microporous Mesoporous Mater.* **2008**, *110*, 232–241.
41. Zukal, A.; Siklova, H.; Cejka, J. Grafting of Alumina on SBA-15: Effect of Surface Roughness. *Langmuir* **2008**, *24*, 9837–9842.
42. Goldbourt, A.; Landau, M. V.; Vega, S. Characterization of Aluminum Species in Alumina Multilayer Grafted MCM-41 Using Al-27 FAM(II)-MQMAS NMR. *J. Phys. Chem. B* **2003**, *107*, 724–731.
43. Larsen, M. R.; Thingholm, T. E.; Jensen, O. N.; Roepstorff, P.; Jorgensen, T. J. D. Highly Selective Enrichment of Phosphorylated Peptides from Peptide Mixtures Using Titanium Dioxide Microcolumns. *Mol. Cell. Proteomics* **2005**, *4*, 873–886.
44. Burgos-Montes, O.; Moreno, R. Stability of Concentrated Suspensions of Al_2O_3-SiO_2 Measured by Multiple Light Scattering. *J. Eur. Ceram. Soc.* **2009**, *29*, 603–610.
45. Gun'ko, V. M.; Zarko, V. I.; Turov, V. V.; Leboda, R.; Chibowski, E.; Pakhlov, E. M.; Goncharuk, E. V.; Marciniak, M.; Voronin, E. F.; Chuiko, A. A. Characterization of Fumed Alumina/Silica/Titania in the Gas Phase and in Aqueous Suspension. *J. Colloid Interface Sci.* **1999**, *220*, 302–323.
46. Bi, H. Y.; Qiao, L.; Busnel, J. M.; Devaud, V.; Liu, B. H.; Girault, H. H. TiO_2 Printed Aluminum Foil: Single-Use Film for a Laser Desorption/Ionization Target Plate. *Anal. Chem.* **2009**, *81*, 1177–1183.